Paper published as:

Tancredi, U.; Renga, A. & Grassi, M. (2013), 'Validation on flight data of a closed-loop approach for GPS-based relative navigation of LEO satellites', *Acta Astronautica* **86**, 126-135.

DOI: 10.1016/j.actaastro.2013.01.005

Validation on Flight Data of a Closed-Loop Approach for GPS-based Relative Navigation of LEO Satellites

U. Tancredi[a]
[a]*University of Naples Parthenope, Centro Direzionale Isola C4, Napoli, 80143, Italy, urbano.tancredi@unipartehnope.it*

A. Renga[b] and M. Grassi[b]
[b]*University of Naples Federico II, P.le Tecchio 80, Napoli, 80125, Italy,*
alfredo.renga@unina.it, michele.grassi@unina.it
ph.:+390817682217 - Fax:+390817682160

This paper describes a carrier-phase differential GPS approach for real-time relative navigation of LEO satellites flying in formation with large separations. These applications are characterized indeed by a highly varying number of GPS satellites in common view and large ionospheric differential errors, which significantly impact relative navigation performance and robustness. To achieve high relative positioning accuracy a navigation algorithm is proposed which processes double-difference code and carrier measurements on two frequencies, to fully exploit the integer nature of the related ambiguities. Specifically, a closed-loop scheme is proposed in which fixed estimates of the baseline and integer ambiguities produced by means of a partial integer fixing step are fed back to an Extended Kalman Filter for improving the float estimate at successive time instants. The approach also benefits from the inclusion in the filter state of the differential ionospheric delay in terms of the Vertical Total Electron Content of each satellite. The navigation algorithm performance is tested on actual flight data from GRACE mission. Results demonstrate the effectiveness of the proposed approach in managing integer unknowns in conjunction with Extended Kalman Filtering, and that centimeter-level accuracy can be achieved in real-time also with large separations.

Keywords: Formation Flying, Relative Navigation, Carrier-based Differential GPS, Vertical Total Electron Content, Integer Ambiguity Estimation, GRACE mission

1 Introduction

In recent years formation flying has attracted the interest of the international scientific community due to the advantages over traditional space systems offered by flying multiple platforms to perform advanced space missions for Earth, universe observation, and gravity field mapping [1-3]. Nevertheless, formation flying requires high levels of relative motion coordination in order to perform common tasks. Autonomous navigation and control is required to fully exploit the advantages offered by flying multiple platforms. Indeed, maintaining specific relative orbital geometries and performing maneuvers as proximity flight or fly around are peculiar aspects of formation flying.

Many applications require the determination of the satellite separations with accuracy at the centimeter level to control the satellite relative positions, especially when they come closer as a result of the relative orbital path, or at the sub-centimeter level to achieve scientific goals [1,2]. For determining the relative position, advanced technologies based on differential GPS and vision and laser systems have been proposed, and a number of missions have been performed for in flight demonstration of these technologies [4]. Whereas laser and vision systems are best suited for close proximity operations, differential GPS techniques can be effectively used for relative navigation with large inter-satellite separations. Of course, accurate relative navigation with the GPS can be only performed in LEO, where the GPS signal strength and the GPS constellation visibility and observation geometry are the most favorable.

Precise relative navigation requires adopting Carrier-phase Differential GPS (CDGPS) techniques which process differential code and carrier-phase measurements [5]. Previous studies focusing on real-time relative navigation of formations in LEO have developed various filtering approaches prevalently for formations of two or more satellites separated of a few kilometers [5,7]. These approaches process double-difference carrier-phase measurements on the L1 frequency within Extended Kalman Filters (EKF), and include in the filter state simplified models of the ionospheric delay to improve estimate accuracy [7]. Numerical and laboratory tests conducted within these works

demonstrate that sub-centimeter level accuracy can be achieved in real time, even if some effects, such as multipath and large Vertical Total Electron Content (VTEC) variations, have not been taken into account. Instead, other studies have achieved similar accuracies for formations with large baselines (> 100 km) only in post-processing [8]. Indeed, for large separations a major technical problem is preserving accuracy and robustness of the integer solution against the increasingly varying number of common-in-view satellites, and ionospheric differential errors.

Only a few studies deal with the real-time relative navigation of large-baseline formations [9, 10]. In these cases measurements on both frequencies are exploited to achieve high accuracy. Nevertheless, performance have been demonstrated on constant baselines only by numerical simulations, using either non linear filtering approaches [9] or complex filter structures based on processing both differenced and un-differenced measurements. Results show that filter performance depends on the baseline, and the filter may diverge for baselines larger than 100 km due to the increasing ionospheric delay error. Finally, it is worth outlining that, to achieve high accuracy, in all the cited works the satellites' absolute orbits are propagated to predict the relative state. This, of course, increases the computation load for real-time applications.

This paper presents a CDGPS-based filtering approach for precise relative navigation of LEO formations with large baselines (in the order of hundreds of kilometers), with computational load compatible with a real-time application. Specifically, a closed-loop navigation scheme is proposed in which the float estimate performed by an Extended Kalman Filter is improved by feeding back the fixed estimates of the baseline and Integer Ambiguities (IA) obtained with a partial integer fixing step. To this end, the proposed approach combines an EKF with the Least-squares AMBiguity Decorrelation Adjustment [11] (LAMBDA) method, which is used for integer ambiguity determination. The management of both real-valued and integer parameters within the same filtering scheme requires the implementation of specific procedures which are also thoroughly analyzed and described in the paper. Approach effectiveness strongly depends on the accuracy of the float ambiguity estimate performed with the EKF, which in turns is affected by the large inter-satellite separation. Thus, to improve the float ambiguity estimate accuracy, double difference ionospheric delay terms are specifically modeled in terms of the VTEC, which is assumed variable over the baseline and introduced in the filter state [12-13]. Finally, the performance of the developed filtering approach is assessed by using real flight data from the Gravity Recovery and Climate Experiment (GRACE) mission, launched in 2002.

The paper is organized as follows: in section 2 the solution approach and the EKF structure are presented, instead sections 3 and 4 describe in detail the proposed navigation scheme and the integer validation strategy; finally results of approach testing on flight data are presented in section 5.

2 EKF-based Real-time Relative Navigation

Precise real-time relative navigation builds upon the exploitation of the integer nature of Double Difference (DD) integer ambiguities. The relative navigation filter must be therefore able to manage both real-value (e.g. relative position and velocity) parameters and integer (DD ambiguities) ones. However, there are no known methods that allow estimating at the same time both real-valued parameters and integer ones. The prominent approaches in geodetic applications (see [14], for instance) perform a float estimate of all parameters, integer ambiguities included, as a first step. This is commonly referred to as the *float* estimate. Then, integer estimates of the cycle ambiguities are obtained applying an integer estimation algorithm to the float estimate. The reliability of this approach is strongly affected by the capability of delivering an accurate float estimate of the integer ambiguities, typically provided by non linear dynamic filters. Large inter-satellite separations (~ 100km) may degrade the accuracy of the float estimate unless highly accurate dynamics and stochastic models are used within the filter. This approach may not be suitable for real time applications, due to the inherent high computational load. Hence, an alternative approach is investigated in this paper able to exploit the integer nature of the DD ambiguity to correct the real-valued float estimate derived by the EKF and thus yielding a *fixed* estimate. The integration of an integer estimation step, based on LAMBDA, with a dynamic filter, such as an EKF, can be interpreted as a solution able to reduce the need for high accuracy dynamic and stochastic models and therefore to guarantee precise real-time relative navigation. The remainder of this section deals with the EKF whereas specific issues relevant to the integration with the LAMBDA method are presented in section 3.

2.1 EKF Process and Observation Models

The relative navigation problem is defined with reference to the ECEF reference frame and a formation of two satellites, named chief and deputy. The problem is described by the following standard nonlinear discrete stochastic model

$$\begin{cases} x_{k+1} = g_k\left(x_k, w_k\right) \\ y_k \quad = h_k\left(x_k, v_k\right) \end{cases} \tag{1}$$

where x is the system state vector, y is the measurement vector, g is the non-linear state propagation function, h is the non-linear observation function, w is the process noise vector, v is measurement noise vector, and the subscript k is used to denote the variable value at the time t_k. Both noises are assumed to be additive, white, Gaussian with zero mean, uncorrelated in time, mutually uncorrelated and uncorrelated with the state vector at the same time sample. The selected state and measurements vector are

$$x \in \mathbb{R}^{(8+2p)\times 1} \ , \ x = \left(\mathbf{b}' \quad \mathbf{VTEC} \quad \mathbf{a}_w \quad \mathbf{a}_1\right)^T \tag{2}$$

$$y \in \mathbb{R}^{4p\times 1} \ , \ y = \left(\mathbf{P}_1^j \quad \mathbf{P}_2^j \quad \mathbf{L}_1^j \quad \mathbf{L}_2^j\right)^T \tag{3}$$

where p is the number of DD observations of each kind. A single difference can be formed by subtracting two undifferenced measurements of the same type and frequency, which are taken by two different receivers at the same time from the same GPS satellite. A double difference can be formed by subtracting two single difference equations of the same type and frequency, which are taken by the same two GPS receivers at the same time from two different GPS satellites, one of which, named pivot, is taken as a reference. Thus the number of available DD observations of each kind is equal to the number of GPS satellites in view of both receivers at the same time, minus one. In Eq.s(2),(3), **b**' stands for the augmented baseline vector (comprising the relative positioning vector from the chief to the deputy and the relative velocity vector), **VTEC** is the vector including the two vertical total electron contents above the receivers, $\mathbf{a}_w$ and $\mathbf{a}_1$ represent the vector of wide-lane and L1 DD ambiguities, respectively. $\mathbf{P}_1^j$ and $\mathbf{P}_2^j$ are DD pseudorange measurement vectors, whereas $\mathbf{L}_1^j$ and $\mathbf{L}_2^j$ are DD carrier phase measurement vectors.

The nonlinear dynamics model foresees Keplerian + J2 relative orbital motion and null nominal (i.e. no errors) dynamics for the other state components

$$\dot{\mathbf{b}}' = f\left(\mathbf{b}'\right) \ , \ \dot{\mathbf{VTEC}} = 0 \ , \ \dot{\mathbf{a}}_w' = 0 \ , \ \dot{\mathbf{a}}_1' = 0 \tag{4}$$

Non-zero process noise is assigned to VTECs and to cycle ambiguities. The selected model has to be interpreted as a trade-off between using a nonlinear model to improve accuracy and having a computational load adequate for real-time implementation. In this way it is possible to get good performance by modeling differential perturbations (e.g. differential drag) as process noise while keeping low the computational effort. Indeed, formation flying satellites usually lie on orbits whose parameters slightly differ and have similar ballistic coefficients so to minimize control efforts to maintain the formation.

As shown in [11], in order to maintain accuracy and robustness in the estimate of double-difference integer ambiguities over large baselines the ionosphere delay terms must be included in the filter state. Specifically, to improve both state vector observability and sensitivity of the dynamic filter baseline variations, double difference ionospheric delay terms are expressed in terms of the VTEC which is then included in the filter state and assumed variable over the baseline. Lear mapping function [15] is used to express the ionospheric delay as a function of VTEC. Actually, the higher correlation [13] between predicted and measured ionospheric delays and precision exhibited by Lear model makes it particularly suited for removing ionospheric delays from DD carrier phase measurements, thus aiding the estimation of the DD integer ambiguities in Extended Kalman Filters for relative navigation over large baselines.

On this basis the nonlinear observation model is given by

$$h : \mathbb{R}^{(8+2p)\times 1} \to \mathbb{R}^{4p\times 1} \quad , \quad y = h(x) \ , \ h(x) = \begin{pmatrix} I_p \\ I_p \\ I_p \\ I_p \end{pmatrix} \boldsymbol{\rho}_{AB}^j\left(\mathbf{b}'\right) + \begin{pmatrix} I_p \\ \gamma^{-2} I_p \\ -I_p \\ -\gamma^{-2} I_p \end{pmatrix} \mathbf{I}_{AB}^j\left(\mathbf{VTEC}\right) + \begin{pmatrix} 0_p \\ 0_p \\ 0_p \\ -\lambda_2 I_p \end{pmatrix} \mathbf{a}_w + \begin{pmatrix} 0_p \\ 0_p \\ \lambda_1 I_p \\ \lambda_2 I_p \end{pmatrix} \mathbf{a}_1 \tag{5}$$

where I_p is the p-dimensional identity matrix, λ_1 and λ_2 are L1 and L2 signal wavelength and $\gamma = \lambda_1 / \lambda_2$ and $\mathbf{I}_{AB}^{j}$ can be derived from Lear mapping function [12]. The observation model relating the state vector to the observables is nonlinear due to the geometric term dependency on the baseline vector.

The Extended Kalman Filter estimates the baseline components, the ionospheric delays (in terms of VTEC for the two satellites) and the DD ambiguities. This is done by applying the Kalman Filter estimation theory to the nonlinear dynamical system defined by Eq.(4) augmented with ambiguities and VTEC terms, and by employing the observation model described by Eq.(5). EKF models and relations can be founded in classic textbooks (see [16,17], for instance), and will not be discussed herein. As mentioned earlier, the EKF is, however, capable of estimating real-valued parameters, and does not take into account that the DD cycle ambiguities are integer. Thus, the EKF yields a *float* estimates, both of the real valued parameters (the baseline, baseline rate and the two VTECs) and of the integer ones. For fully exploiting the high accuracy of the carrier phase measurements, the DD ambiguities must be fixed to their integer values, and the float solution updated to reflect this change, yielding the *fixed* solution.

3 Relative Positioning Approach

The LAMBDA [11] method is used to conduct the integer fixing step. This is an Integer Least Squares (ILS) estimator searching for the optimum integers into a transformed integer space. More specifically, LAMBDA applies the so-called Z-transformation. Z-transformation has the property of preserving the integer nature of the ambiguities while heavily decorrelating the ambiguity vector components, which results in a more efficient way of determining the ILS solution. As a result, LAMBDA outputs the integer estimate of DD ambiguities. However, LAMBDA does not provide a stochastic characterization of those estimates thus complicating the integration with EKF results.

A practical solution is to assume the integer estimates generated by LAMBDA to be deterministic. This approach is not fully justified from a theoretical point of view. In practice, the IA estimated by LAMBDA could be considered deterministic if the float estimates of the ambiguities are unbiased and their distribution is sufficiently sharp about the (integer) mean [14]. This does not happen in real world data, where the float distribution can be biased and converge to a non-integer value. In order for ascertaining if this is the case, validation tests must be used. Validation tests will be analyzed in the following section, while the remainder of this section specifically deals with different schemes for correcting real-valued float estimate to obtain fixed estimates based on the fixed (and validated) ambiguities.

There are three main approaches that have been applied in problems that show similarities with the application considered in the present paper. The simplest approach is to disregard the integer nature of the DD carrier phase ambiguities. This has been proved to work for relative positioning with centimeter accuracy [5,18] , but for relatively short baselines of the order of 1 km and not using real-world GPS measurements. As such it is not suitable for long-baseline applications.

As an alternative, an integer-fixing algorithm, such as LAMBDA, can be used to fix the integer values of the ambiguities using their float estimates. In case enough ambiguities are fixed to integers, the float baseline can be corrected for obtaining a sharper "fixed" estimate. This step can be carried out exploiting the estimates of the cross-correlation between the float baseline and the float ambiguities. Indeed, when the ambiguities are successfully fixed, the error affecting the float ambiguities is known (i.e. is the difference of fixed and float values). Thus, the error on the float baseline can be estimated and compensated, yielding the fixed baseline. Let us consider a state vector x, in which the baseline vector b comprises all real-valued component of the state x (i.e. the baseline, the baseline rate and the two VTECs in our case) and the integer vector a includes both WL and L1 carrier-phase ambiguities. Denote by a circumflex accent the float estimate, by a breve accent the fixed estimate, and by P_{cd} the covariance matrix between two generic vector variables c and d. The fixed baseline is related to the float one and to the fixed integer ambiguities as follows [14]:

$$\breve{b} = \hat{b} + P_{ba} P_{aa}^{-1} \left(\breve{a} - \hat{a} \right) \; ; \; P_{b|\breve{a}} = P_{bb} - P_{ba} P_{aa}^{-1} P_{ab} \tag{6}$$

Thus, Eq.(6) allows improving the baseline accuracy beyond that of a purely float approach. One can imagine to let a dynamic filter (e.g. an EKF) run undisturbed and provide a float estimate of the baseline and of the DD ambiguities. An integer-fixing algorithm, such as LAMBDA, tries to fix the integer values of the ambiguities based on the float estimate. Integer validation tests might be used to increase the probability of correct IA estimation, by accepting only promising LAMBDA solutions. This corresponds to the "open-loop" approach depicted in Figure 1. It has been applied in several relative kinematic positioning applications [9,19–21], including relative spacecraft positioning. However, this approach requires that the float ambiguities estimates are sufficiently close to the exact integer. If this is not the case, either numerous LAMBDA solutions will be rejected by the validation tests or cycle

ambiguity errors will be incorporated into the fixed baseline via Eq.(6), thus degrading the overall accuracy of the estimated baseline.

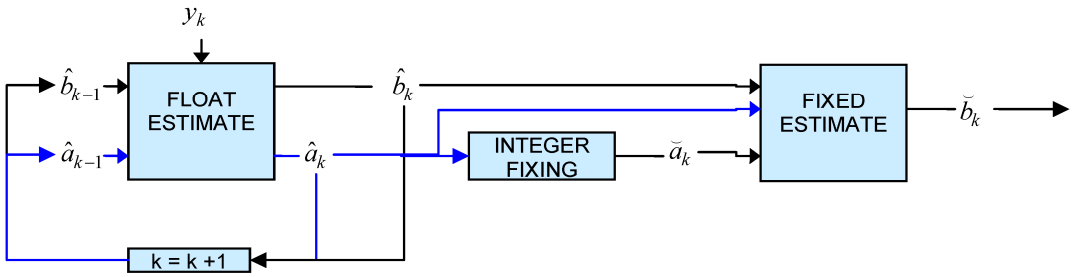

Figure 1. Open-loop baseline fixing approach flow diagram.

As an alternative to the approach of Fig.1, many references in spaceborne GPS receivers applications [8,22–28] do exploit the knowledge of the fixed integer ambiguities and the fixed baseline estimate (with the relevant covariance matrix) as feedback signals for improving the float estimates in the following time instants. In practice, Eq.(6) is used at a certain time epoch not only for obtaining the fixed solution, but also for modifying the EKF state vector and covariance matrix. Note that some authors [8,22–23] propose a pseudo-measurement step for implementing this update of the state vector. By carrying out Kalman filter's algebra, it is easy to verify that these pseudo-measurement steps are equivalent to Eq.(6). This approach, which feeds back the fixed estimates to the EKF, can be viewed as a "closed-loop" scheme, and is depicted in Figure 2.

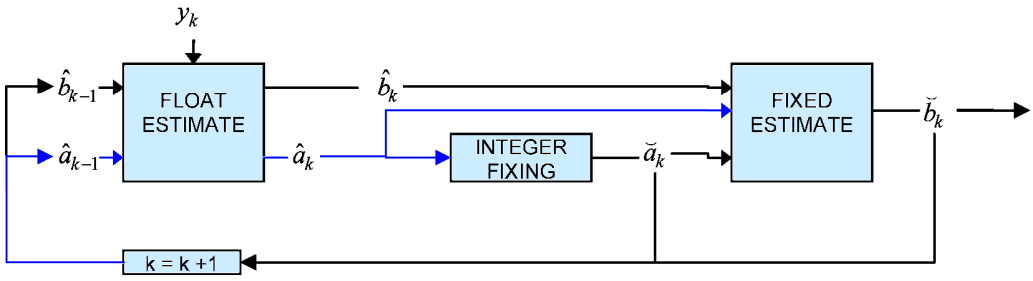

Figure 2. Closed-loop baseline fixing approach flow diagram.

For completeness it is important to point out that in [8] a comparison has been conducted between an open-loop solution and its closed-loop one, showing that the open-loop solution is not capable of performing as the closed loop one. Its performances were found to be somehow in between the float and the closed loop approaches. From these considerations, it is possible to conclude that the aiding of the float estimate with the integer fixing step results is necessary in long-baseline application as the present one. This claim is also supported by [22], which states that in the absence of such state-vector updates (by means of the fixed integer ambiguities) orbit solutions converge only with precise initialization and dynamics modeling.

The selection of a closed-loop approach requires the implementation of proper strategies to manage integer fixing/validation steps within the EKF, that is, which ambiguities continue to keep in the filter state and to feed LAMBDA and the validation step. First of all, following the results shown in [8,22,25], it seems advisable to foresee a capability of partial integer fixing, i.e. being capable of fixing only a subset of the float ambiguities when validation of the whole set, i.e. vector integer validation, fails (see next section for the details). Thus, the navigation algorithm will deal with a mixed array of fixed and un-fixed ambiguities, representing both not yet validated ambiguities and ambiguities related to newly acquired satellites. The overall logic of the navigation algorithm can be summarized as in Figure 3. In this scheme, only a subset $\breve{a}_k$ of the float ambiguities $\hat{a}_k$ is fixed, leaving the other non-validated ambiguities $\hat{a}'_k$ as float estimates. Once the fixed ambiguities $\breve{a}_k$ are used for updating the float variables vector $\hat{b}'_k = \begin{pmatrix} \hat{b}_k & \hat{a}'_k \end{pmatrix}$ into the fixed one $\breve{b}'_k$ by Eq.(6), they become uncorrelated with the fixed baseline, and can be dropped from the EKF state vector. Their fixed value will be then used only for unbiasing the relevant DD carrier phase measurements, which become highly accurate pseudorange measurements, until one of the two GPS satellites forming the DD couple is lost.

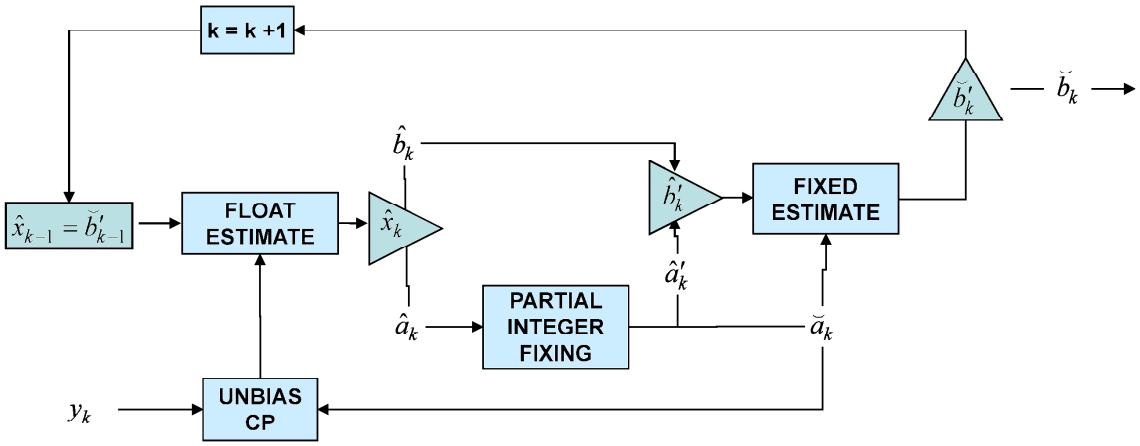

Figure 3. Proposed Algorithm Logic: Flow Diagram

Finally, it is worth noting that Eq.(6) updates the inter-satellite distance, the relative velocity and ionospheric delays through VTECs. The final baseline accuracy is then also limited by the accuracy of VTEC-based ionospheric model (and Lear mapping function too). As shown in [12], the VTEC-based model is accurate enough to aid integer ambiguity resolution, but it can be unsatisfactory to correct the baseline estimate (especially over polar areas) once integer ambiguities have been fixed and validated. For this reason, the fixed ambiguities are used for performing a refinement of the EKF solution. More precisely, when the fixed integer ambiguities allow for obtaining more than 3 ionospheric-free combinations of the unbiased carrier phase measurements, a kinematic filter, based on a Weighted Least Square (WLSQ) algorithm processing such ionospheric-free combinations, is applied to refine the baseline estimation.

4 Integer Ambiguity Validation Strategy

Different strategies are available to perform integer ambiguity validation. The classical approach is to test if all the integer ambiguities are simultaneously valid. These "vector" validation tests operate on the whole vector of integer ambiguities, and do not discriminate between ambiguities within the vector: if only one ambiguity within the vector is deemed erroneous, the whole vector does not pass the test. An example of vector validation test is the so-called Minimum Required Success Rate [8,14] that computes the theoretical success rate of the integer ambiguity, and does not require the integer estimate LAMBDA . This test could thus be useful for deciding if the computation burden needed for running LAMBDA is worth being spent, or if the expected outcome is unlikely to be useful in any case. Other validation tests exist, but they all lack a sound theoretical basis (see [14] for a detailed discussion of this topic).

A potential alternative is represented by the so-called Integer Aperture estimators [14]. Unlike classical integer estimators that always provide an integer solution, regardless of the quality of the float estimate, Integer Aperture estimators explicitly consider that in some cases it is better not to fix the float estimate. [14] proves that the classical integer estimator followed by a validation step belong to the class of Integer Aperture. An important limitation of the Integer Aperture estimators is that the value of the "aperture parameter", which plays the role of the threshold acceptance values in validation tests, is difficult to compute rigorously. The aperture parameter is determined by Monte Carlo simulation in most cases, which prevents considering Integer Aperture estimators from being used in real-time applications.

On the other hand, when not all the integer ambiguities are correctly fixed, there is the possibility that a subset of the integer ambiguity vector is instead correct. Partial integer ambiguity validation tests are concerned with discriminating between the single ambiguities, i.e. separating the correct from the incorrect ones. Concerning this, it is well-known that wide-lane integer ambiguities are more easily estimated than other ambiguities by any integer ambiguity estimator thanks to their wavelength, which significantly exceeds the typical pseudorange measurement error. In addition, the results presented in [29] suggest that the most accurate LAMBDA estimate is equal to the wide-lane one when the ionosphere error contribution is higher than the measurement noise. This result allows claiming also that the wide-lane ambiguities estimates have almost uncorrelated variance, which further strengthens the theoretical consistency of partial validation tests.

According to this analysis only partial integer ambiguity validation tests are taken into account and implemented in the algorithm logic reported in Figure 3. More in detail, first wide-lane float ambiguities are tested, and only for those DD couples with a validated wide-lane ambiguity additional tests are performed to validate also L1 integer ambiguities.Wide-lane ambiguities are validated only if the following two tests are passed:

- Float wide-lane ambiguity residuals [8]
- Instantaneous residuals of Melbourne-Wubbena (MW) observables [30,31]

The first test evaluates the difference between the float estimate of the wide-lane ambiguity and its integer one. In practice, a threshold is introduced as the maximum difference under which an integer value is deemed correct. The second test checks the residual of Melbourne-Wubbena observables representing a direct, unbiased but noisy, measure of wide-lane integer ambiguities. It is worth noting that the first test is strongly influced by EKF float estimate of integer ambiguities while the second one only depends on pseudorange and carrier phase measurements. The combination of these tests can potentially reduce the probability that a bias in the float estimate of the ambiguity lead to the validation of wrong integer ambiguities.

In order to validate the integer estimate of L1 ambiguities, for all the DD couples passing the former two tests, two additional tests are performed:

- Distance between the float and the integer value of narrow-lane combinations [16] of wide-lane and L1 integer ambiguity
- Instantaneous residuals on ionospheric-free DD carrier-phase measurements [8]

Again the first test is dominated by the EKF float estimates of integer ambiguities, whereas the second one is affected also by the baseline estimate and carrier-phase measurements.

5 Approach Test on Flight Data

The performance of the proposed approach is evaluated using actual flight data from spaceborne GPS receivers. According to the previous sections, evaluation of the models is of interest for two receivers flying in formation and separated by a large baseline, in the order of hundreds of km. Flight data matching these requirements is made available by the Gravity Recovery and Climate Experiment (GRACE) mission, launched in 2002. An overview of the GRACE mission can be found in [32]. It consists of two identical satellites, GRACE A and GRACE B, in near circular orbits at an initial altitude of approximately 500 km and 89.5 deg. inclination. The satellites are nominally separated of 220 km in the along track direction. The primary mission objective is to map the Earth's gravity field, which is accomplished by the mission's key instruments, the Ka-Band Ranging System (KBR) and high-precision accelerometers. Each spacecraft is also equipped with identical NASA JPL BlackJack GPS receivers [33]. A post-processed version of GRACE data, known as Level 1B (L1B) data, is made available to the scientific community by JPL's Physical Oceanography Distributed Active Archive Center (PODAAC). The Level 1B data are derived from the processing applied to the raw data described by [34].

A specific dataset has been selected from all available GRACE L1B data for the analysis presented in this paper. The dataset refers to January 14th, 2009, in which GRACE B leads the formation and GRACE A follows at a distance of 266 ± 1.8 km and the orbit altitude ranges between ~450 km and ~480 km during the day, which yields an orbital period of about 1 hour 34 minutes. This data set is representative of a formation of two satellite with a large separation. Indeed, the maximum separation between the two GRACE satellites is expected to be about 270 km. The selected dataset comprises 5 complete orbital revolutions of the GRACE satellites. Because GPS receivers' L1B data are available at a sampling rate of 0.1 Hz, this results in more than 2800 samples. GPS L1B data used by the filter consists of two pseudorange measurements and two carrier phase measurements from code observations on the L1 frequency and semi-codeless tracking on the L2 frequency. As with all GRACE Level 1B data, the time-tags are corrected to GPS time using GPS clock solutions computed in post-processing [35]. A data-editing step, compatible with real-time implementation, has been performed on GPS L1B data, in order to detect and remove outliers in the pseudorange measurements and to discard all observations from GPS satellites whose elevation above the local horizon is smaller than 10 deg.

The relative navigation filter estimation performances are quantified by comparing the baseline estimated by the filter to a reference solution provided as part of GRACE L1B data. In particular, KBR data have been used for assessing the accuracy in determining the baseline magnitude. The KBR instrument measures the change in distance between the spacecraft, also known as the biased range, with a precision of 10 μm. The biased range can be seen as the true range plus an unknown bias. The bias is arbitrary for each piecewise continuous segment of phase change measurements and has to be compensated by a specially designed procedure, described in detail by [8]. The Level 1B data includes also a GPS Navigation (GNV) data product, which contains an estimate of the two spacecraft Center of Mass (CoM) position and velocity vectors. These estimates are obtained as a product of a precision orbit determination

tool [34] and typically have a time-varying accuracy of a few centimeters in position. Both KBR and GNV data allow estimating the baseline between the spacecraft CoM, whereas GPS measurements allow reconstructing the baseline between the two GPS antennas. Therefore, the GPS antenna offset w.r.t. the CoM is compensated when necessary taking into account each spacecraft attitude, which is provided in GRACE L1B data as well. For providing additional insight into the filter performances, its capability of fixing the correct integer ambiguities is also analyzed. For this purpose, reference values of all integer ambiguities have been obtained. These reference ambiguities are computed taking advantage of the knowledge of the observation geometry given by the KBR and GNV data. The procedure is described in [13], to which we refer the interested reader.

The proposed relative navigation filter has been run on the selected dataset. Numerical simulation of the complete data took less than 2 minutes to be completed in Matlab®, (in face of a simulated time span of ~ 8 hours) on a standard desktop PC equipped with a Pentium IV 2.4 GHz processor and 2GB RAM. For having an indication of how these execution times scale when the algorithm is run on a different machine, such as a real-time onboard computer for space applications, the FLoating point OPerations per Second (FLOPS) necessary to the relative navigation algorithm are also estimated. More precisely, the FLOPS required to run the algorithm continuously on the 8-h dataset are estimated based on the computing power of the above PC, on the algorithm's execution time, and on the dataset duration, yielding an average value of ~ 40 MFLOPS. This value is fully compatible with state-of-the-art, space-qualified CPUs (e.g. [36]). It shall be also considered that the algorithm is implemented in MATLAB with virtually no software coding optimization. This implies that the FLOPS strictly necessary to the algorithm for computing the baseline are probably significantly less. All the above considerations suggest that the computational load is adequate for providing real-time relative positioning.

Figure 4 shows the percentage of integer ambiguities which are fixed by the filter w.r.t. the total number of available ambiguities at each time epoch. The filter is capable of fixing almost the 90% of the total ambiguities in the selected dataset, 88.4% of WL ambiguities and 86.1% of L1 ambiguities, with zero fail rate. It is apparent, however, that there are several time intervals in which the ambiguity fixing percentage drops down significantly. In these time epochs, the number of iono-free combinations of unbiased carrier phase measurements is lower than four, implying that the kinematic correction cannot be applied to refine the EKF results. It is outlined that the null fail rate for both WL and L1 ambiguities implies that the validation tests do not allow passing any incorrect ambiguity. This feature is crucial for establishing the performance of the proposed filter, and, more broadly, of filters arranged in the closed-loop scheme presented in Figure 2. Indeed, an erroneously fixed integer ambiguity will worsen the filter capability of estimating the remaining ambiguities in the subsequent time epochs, further decreasing the estimation accuracy as more integer ambiguities become erroneously fixed, possibly leading to divergence of the solution. However, the presence of the MW validation test limits the magnitude of these divergence phenomena, thanks to the independence from the filter estimates of MW combinations.

Figure 5 shows the baseline magnitude estimation error, obtained comparing the filter's solution to the highly accurate KBR one. The time epochs in which the kinematic correction is not available are highlighted in red. Thanks to the IA fixing performances, the kinematic correction is available in more than 85 % of the time epochs. Results also confirm that the kinematic correction is useful in refining the EKF solution. Despite a baseline of more than 250 km, the baseline magnitude is estimated with a RMS error of about 3.4 cm. and the maximum error is below 20 cm.

The baseline vector estimation performances are plotted in Figure 6 together with the 3σ bounds predicted by the navigation filter (shown as the shaded gray area). Note that the baseline estimation error is obtained using the GNV data products as a reference. These have a typical accuracy of a few centimeters, which is comparable to the baseline estimation error order of magnitude. From this perspective, these results are less significant than the ones presented for the baseline magnitude. Figure 6 depicts the baseline error components in the Orbital Reference Frame (ORF), whose x axis is directed along-track, its y-axis is directed cross-track, and the z one is in the radial direction. The relative navigation performances are higher in the cross-track direction and worse in the radial one, due to GPS observation geometry. Nonetheless, all three components are estimated with a RMS error in the order of few centimeters, and almost always smaller than 20 centimeters. Moreover, the filter predicts an error variance that is consistent with the actual error, confirming the robustness of the filter estimates.

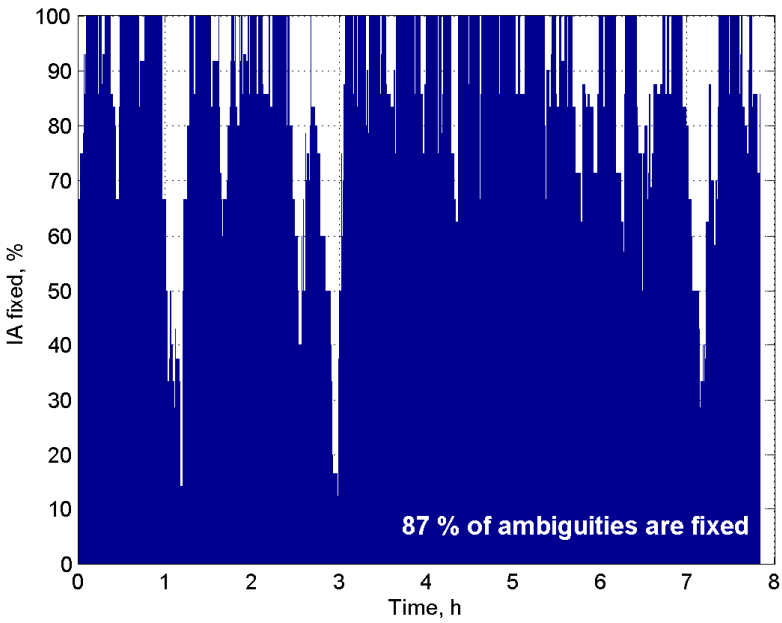

Figure 4 Percentage of Integer Ambiguities (IA) fixed by the filter

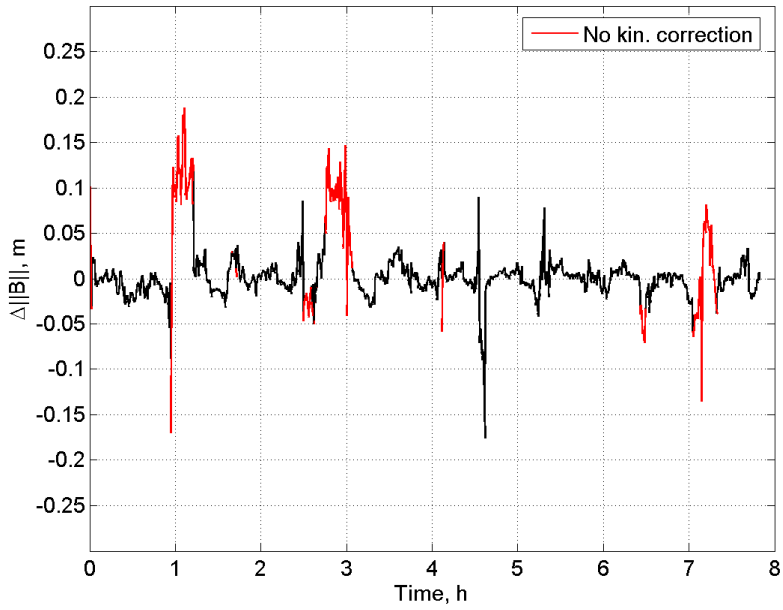

Figure 5 Baseline magnitude estimation error

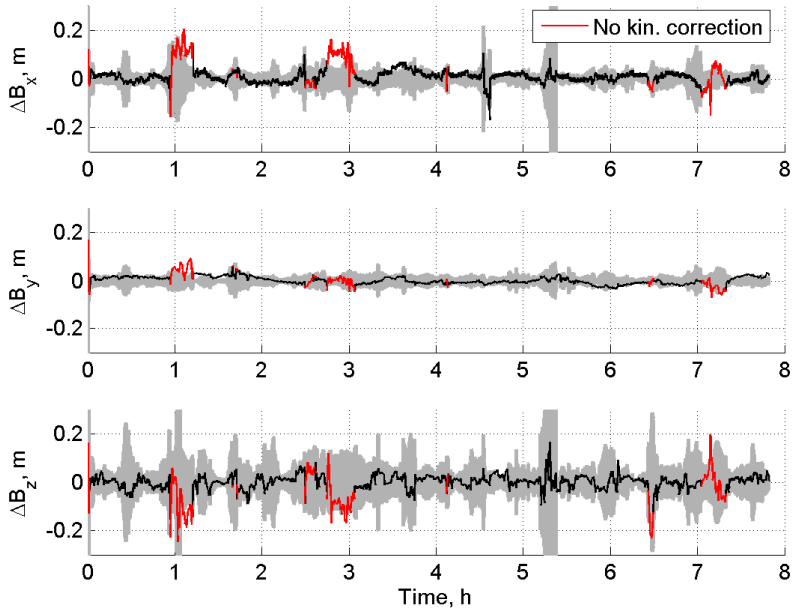

Figure 6 Baseline estimation error in ORF. Gray shaded area stands for ±3σ bounds predicted by the filter.

The relative navigation performances are summarized in Table 1.

Table 1. Relative Navigation Performances

Baseline Component	Estimation Error	
	Max, cm.	*RMS, cm.*
Magnitude (||B||)	18.8	3.4
Along Track (B_x)	20.4	3.8
Cross Track (B_y)	16.8	1.9
Radial (B_z)	24.6	4.4
Kin. Correction Availability	85.6 %	

6 Conclusion

A filtering approach relying on Carrier-based Differential GPS for relative navigation of LEO formations with large inter-satellite separations has been presented. Approach requirements are real-time operation and precise baseline determination. To this end the proposed navigation algorithm adopts a simplified nonlinear model of the satellite relative dynamics and exploits the integer nature of the double-difference carrier-phase ambiguities.

A major technical problem when dealing with large baseline formations is preserving accuracy and robustness of integer ambiguity solution against the increasingly varying number of common-in-view satellites and large ionospheric differential errors. To overcome limitations of the adopted relative dynamics model and problems caused by the large inter-satellite separation, the proposed navigation filter adopts a closed-loop scheme in which fixed estimates of the baseline and integer ambiguities, obtained with a partial integer fixing step, are fed back to an Extended Kalman Filter in order to improve the float estimate at successive time instants. To manage both real-valued, including double-difference ionospheric terms, and integer parameters, the navigation filter integrates the Extended Kalman Filter with an Integer Least Squares estimator based on the LAMDBA method. In addition, different tests are performed to effectively validate such integer estimates.

Filter performance has been evaluated on actual flight data from spaceborne GPS receivers. Flight data from the GPS receivers on board the Gravity Recovery and Climate Experiment (GRACE) mission, launched in 2002, have

been used. GRACE consists of two satellites flying in a leader-follower formation. The analyzed data set is relevant to a condition of maximum separation between the two satellites (about 270 km), which is of interest for testing the relative navigation approach presented in the paper.

Results show that the proposed filtering scheme is able to fix almost the 90% of the total ambiguities in the selected dataset, being also able to recognize and discard wrong estimates of integer ambiguities. This performance is, of course, crucial to get an accurate baseline determination. As a consequence, despite the inter-satellite large separation (about 266 km), the baseline components are estimated with RMS errors between 2 cm and 4.5 cm and maximum errors between 17 cm and 25 cm, being the errors higher in the radial components. Finally, the comparison of the time required by numerical simulation of the complete data set (about 2 minutes) with the simulated time span (about 8 hours) suggests that the computational load is adequate to using the proposed approach in real-time applications.

7 Acknowledgements

This work has been carried out with the financial contribution of Regione Campania within the framework of the of the project for Technology Innovation of Transport Systems (INSIST).

8 References

1. M. D'Errico, and A. Moccia, The BISSAT mission: a bistatic SAR operating in formation with COSMO/SkyMed X-band radar, Aerospace Conf. Proceedings, IEEE, 2 (2002) 2/809-2/818
2. G. Krieger, et al., TanDEM-X: A Satellite Formation for High-Resolution SAR Interferometry, IEEE Trans. on Geoscience and Remote Sensing, 45 (2007) 3317-3341
3. C. V. M. Fridlund and F. Capaccioni, Infrared space interferometry- the DARWIN mission, Advances in Space Research, 30 (2002) 2135-2145
4. S. Persson et al., Prisma – An Autonomous Formation Flying Mission, ESA Small Satellite Systems and Services Symposium (4S) September 2006, Sardinia, Italy, 25-29
5. Bondavalli, A., Ceccarelli, A., Gogaj, F., Seminatore, A., Vadursi, M. Experimental assessment of low-cost GPS-based localization in railway worksite-like scenarios (2013) Measurement: Journal of the International Measurement Confederation, 46 (1), pp. 456-466.
6. T. Ebinuma, et all, Integrated Hardware Investigations of Precision Spacecraft Rendezvous Using the Global Positioning System, Journal of Guidance, Navigation and Control, 26 (2003) 425-433
7. S. Leung and O. Montenbruck, Real-Time Navigation of Formation-Flying Spacecraft Using Global-Positioning-System measurements, Journal of Guidance, Control and Dynamics, 28 (2005) 226-235
8. R. Kroes, Precise relative positioning of formation flying spacecraft using GPS, Ph.D. Thesis, Delft University of Technology, The Netherlands, 2006.
9. Jonathan D. Wolfe et all, Estimation of Relative Satellite Position Using Transformed Differential Carrier-Phase GPS Measurements, Journal of Guidance, Control and Dynamics, 30 (2007) 1217-1227
10. W.A. Bamford Jr., Navigation and Control of Large Satellite Formations, Ph.D Dissertation, The University of Texas at Austin, USA, 2004
11. P. de Jonge and C. Tiberius, The LAMBDA method for integer ambiguity estimation: implementation aspects, LGR-Series Publications of the Delft Geodetic Computing Centre, 12 (1996)
12. U. Tancredi, A. Renga, M. Grassi, GPS-based Relative Navigation of LEO formations with Varying Baselines, Proc. Of AIAA Guidance Navigation and Control Conference, Toronto, Canada, August 2010
13. U. Tancredi, A. Renga, M. Grassi, Ionospheric path delay models for spaceborne GPS receivers flying in formation with large baselines, Advances in Space Research, 48 (2011) 507–520
14. S. Verhagen, The GNSS integer ambiguities: estimation and validation, Ph.D. Thesis, Delft TU, 2005
15. W.M. Lear, GPS navigation for low-earth orbiting vehicles, NASA Lyndon B. Johnson Space Center, Mission planning and analysis division, 1st revision, NASA 87-FM-2, JSC-32,031, 1988
16. J. Farrel and M. Barth, The Global Positioning System and Inertial Navigation, McGraw-Hill, New York, 1999, ch. 5
17. A. Gelb, Applied Optimal Estimation, Cambridge, USA, The M.I.T. Press, 1974
18. F.D. Busse, Precise Formation Estimation in Low Earth Orbit Using GPS, Ph.D. Dissertation, Stanford University, USA, 2002
19. D. Odijk, J. Traugott, G. Sachs, O. Montenbruck, C. Tiberius, Two Approaches to Precise Kinematic GPS Positioning with Miniaturized L1 Receivers, Proceedings of the 20th International Technical Meeting of the Satellite Division of The Institute of Navigation (ION GNSS 2007), Fort Worth, USA, (2007) 827-838
20. D. Kim and R.B. Langley, A Reliable Approach for Ambiguity Resolution in Real-time Long-baseline Kinematic GPS Applications, Proc. of ION GPS 2000, 13th International Technical Meeting of the Satellite Division of The Institute of Navigation, Salt Lake City, USA, (2000) 1081-1091
21. Duncan B. Cox, Jr. and John D. W Brading, Integration of LAMBDA Ambiguity Resolution with Kalman Filter For Relative Navigation of Spacecraft, Navigation, 47 (2000) 205-210

22. S-C.Wu and Y.E. Bar-Sever, Real-Time Sub-cm Differential Orbit Determination of Two Low-Earth Orbiters With GPS Bias Fixing, Proc. of the 19th International Technical Meeting of the Satellite Division of The Institute of Navigation (ION GNSS 2006), Fort Worth, USA, (2006) 2515-2522
23. R. Kroes, O. Montenbruck, W. Bertiger, P. Visser, Precise GRACE baseline determination using GPS, GPS Solutions, 9 (2005) 21–31
24. A. Hauschild, O. Montenbruck, GPS-Based Attitude Determination for Microsatellites, Proc. of the 20th International Technical Meeting of the Satellite Division of The Institute of Navigation (ION GNSS 2007), Fort Worth, USA, (2007) 2424-2434
25. L. Dai, D.Eslinger, T. Sharpe, Innovative Algorithms to Improve Long Range RTK Reliability and Availability, Proc. of the 2007 National Technical Meeting of The Institute of Navigation, (2007) 860-872
26. S. Mohiuddin, M.L. Psiaki, Carrier-Phase Differential Global Positioning System Navigation Filter for High-Altitude Spacecraft, AIAA Journal of Guidance, Control, and Dynamics, 31 (2008) 801-814
27. M. L., Psiaki, Kalman Filtering and Smoothing to Estimate Real-Valued States and Integer Constants, AIAA Journal of Guidance, Control, and Dynamics, 33 (2010) 1404-1417
28. T. Takasu and A. Yasuda, Kalman-Filter-Based Integer Ambiguity Resolution Strategy for Long-Baseline RTK with Ionosphere and Troposphere Estimation, Proc. of the 23th International Technical Meeting of The Satellite Division of the Institute of Navigation (ION GNSS 2010), Portland, USA, (2010) 161-171.
29. P.J.G.Teunissen, P. Joosten and C.C.J.M. Tiberius, Geometry-free ambiguity success rates in case of partial fixing, Proc. of National Technical Meeting & 19th Biennal Guidance Test Symposium ION, (1999) 201-207
30. W.G. Melbourne, The case for ranging in GPS-based geodetic systems, in Proceedings of the 1st Intenational Symposium on Precise positioning with the Global Positioning System, Rockville, Maryland, USA, (1985) 373–386
31. G. Wubbena, Software developments for geodetic positioning with GPS using TI 4100 code and carrier measurements, Proc. of the 1st Intenational Symposium on Precise positioning with the Global Positioning System, Rockville, Maryland, USA, (1985) 403–412
32. B. D. Tapley, S. Bettadpur, M. Watkins, C. Reigber, The gravity recovery and climate experiment mission overview and early results, Geophys. Res. Lett., 31, L09607 (2004)
33. G. Davis, E. Davis, S. Luthcke, K. Hawkins, Pre-Launch Testing of GPS Receivers for Geodetic Space Missions, Proc. of the 13th International Technical Meeting of the Satellite Division of The Institute of Navigation, Salt Lake City, USA, (2000) 2009-2018
34. S.C. Wu, G. Kruizinga, W. Bertiger, Algorithm theoretical basis document for GRACE level 1B data processing, NASA Jet Propulsion Laboratory, revision 1.2, JPL D-27672, GRACE 327-741 (2006)
35. K. Case, G. Kruizinga, S.C. Wu, GRACE level 1B data product user handbook, NASA Jet Propulsion Laboratory, revision 1.3, JPL D-22027, GRACE 327-733 (2010)
36. Anonymous, Proton200k™ Radiation Hardened Single Board Computer for Space Applications Datasheet, v.4.0, SpaceMicro Inc., available at: http://www.spacemicro.com/pdfs/Proton200k-DSP_Datasheet_v4.0.pdf (last retrieved on January 8, 2013)